DESIGN AND FABRICATION OF MOVABLE SILICON PLATES SUSPENDED BY FLEXIBLE SUPPORTS

Mark G. Allen, Martin Scheidl, and Rosemary L. Smith*
Microsystems Technology Laboratories
Massachusetts Institute of Technology
Cambridge, MA 02139

* Present address: Department of Electrical Engineering and Computer Science
University of California at Davis, Davis, CA

ABSTRACT

A process for fabricating silicon plates of varying thicknesses suspended by thin, flexible polyimide arms has been developed. The process uses bulk micromachining techniques and consists of four steps: a diaphragm etch from the back of the wafer, a trench etch from the front side (to define the plates), deposition and patterning of the plate support beams, and a self-aligned backside plasma etch to release the plates. We have used this process to fabricate square silicon plates two millimeters on a side and 7-10 μm thick suspended by polyimide beams 500 μm long, 4 μm thick, and 100-200 μm wide. By evaporating aluminum on the topside of the plates, it was possible to deflect them electrostatically approximately 60 μm at 40 V applied voltage. These structures were designed for application as micromachined mirrors, although their sensitivity to motion and electrical and thermal isolation suggest other potential applications such as gas sensors, flow sensors, and accelerometers.

INTRODUCTION

The technique of micromachining has been used to make a host of movable and flexible structures for sensing and actuation purposes (see, e.g., [1-3]). Recently there has been interest in deflectable reflecting plates for use as mirrors in fiber optic switching and display applications [4-7]. As many of these structures are micromachined from silicon, and as silicon is a stiff material, relatively large driving voltages may be required for large motions. In this work we have used silicon plates supported by flexible polyimide beams in the hope of reducing the driving forces required for large-scale deflection.

Structures using polyimide-supported plates as thermally isolated structures for gas sensors have been described by Stemme [8]. In that structure, polyimide was chosen for its thermal, not mechanical, properties. More recently, there has been much work in characterization of polyimide for use as structural members in microsensors and microactuators [9-10]. Quantitative knowledge of the Young's modulus, residual stress, and debond energy (adhesion) have permitted the design and fabrication of microsensors using this material. Other desirable properties of polyimide are its mechanical flexibility (relative to silicon), its planarization properties, and its compatibility with integrated circuit processing. This paper will describe the design, fabrication, and testing of square silicon plates suspended by polyimide beams of various configurations, discuss the movement of these plates using electrostatic drive, and describe the voltage-deflection characteristics of these structures using a simple electromechanical model.

DESIGN

The following goals were used in the initial structure design. First, the plate itself must be mechanically stable; that is, it cannot buckle or bend unacceptably due either to outside loading or intrinsic stress in the plate, various films on top of the plate, or the plate supports. In effect, this sets a lower limit on the plate thickness. Second, the plate be able to rotate four degrees from the horizontal at reasonable electrostatic drive voltages but not sag unacceptably under its own weight. A maximum drive voltage of 100 V from a distance of 300 μm and maximum sag of 0.5 degrees at 0V were selected. Finally, the shape and minimum size of the plate was selected to be a square two millimeters on a side. In order to meet all these design criteria, it was decided to use a the two-material system described above for fabricating the structure. Bulk silicon was chosen for the plate due to its stiffness and relative lack of internal stresses (as compared with deposited films). Polyimide was chosen as the beam/support material for the reasons described above: it is compatible with integrated circuit processing, it has a relatively low modulus of elasticity compared to silicon (and thus is relatively flexible), its mechanical properties have been well characterized, and it has excellent planarizing properties.

The beam configurations chosen for supporting the silicon plates are shown in Figure 1 [11]. As can be seen, there are three different beam designs. The first, shown in Fig. 1a, is called the end torsional configuration. The polyimide beam is located at the end of the plate and is loaded in torsion when the plate deflects into the page. The second, called the center torsional configuration (Fig. 1b), is identical to the end torsional device except that the supporting beam is located in the center of the plate. This allows a 'back and forth' motion of the plate (in and out of the page) in response to a differential driving force. Finally, the third design is called the bending configuration (Fig. 1c). In this structure, the polyimide beams are loaded in bending when the plate deflects into the page. The beam widths and thicknesses chosen to meet the above design goals are shown beneath each structure in Figure 1; calculation of these quantities is detailed in reference [11].

TH0249-3|89|0000|0016$1.00©1989 IEEE

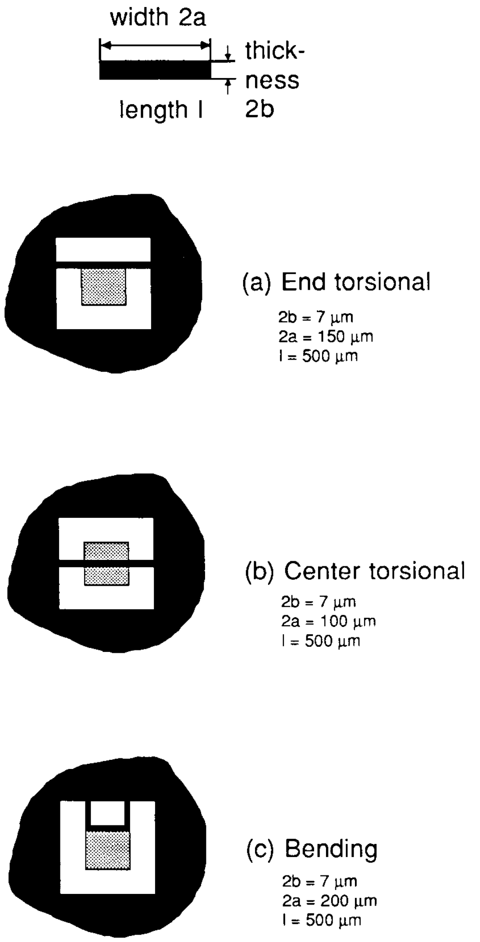

Figure 1. Beam types and design parameters

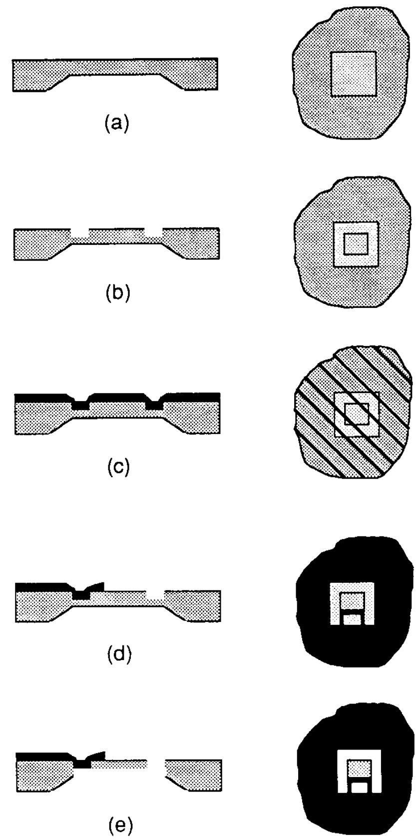

Figure 2. Process sequence (bending beam design)

FABRICATION

The flexibly supported plates were fabricated using standard bulk micromachining techniques. The starting material was a single-side polished <100> n-type silicon wafer two inches in diameter and 11 ± 1 mils thick. A 1.3 μm thick masking oxide was grown at 1100 °C in steam for three hours. The front of the wafer was protected with photoresist and the oxide on the backside of the wafer was patterned into a series of square holes 3 millimeters on a side using a buffered oxide etch (BOE) (see Figure 2). The photoresist was stripped in 3:1 sulfuric acid:hydrogen peroxide solution and the wafers were etched in 20% by weight potassium hydroxide (KOH) solution at 56 °C for 11 hours. The etch rate of this solution was 20-21 μm/hr forming 3 mm square diaphragms approximately 50 μm in thickness (Fig. 2b). The front side oxide was then patterned and etched in the above KOH solution for 30 minutes to form trenches 10 μm deep (Fig. 2c). At this point, the etched wafers could be cleaned and used to build electronic devices adjacent to and/or integrated with the plates, although this was not done for the initial study reported here. The masking oxide was stripped in BOE and an adhesion promoter layer consisting of a 0.5% solution of γ-triethoxyaminopropylsilane in 95% methanol/5% water was spin-coated on the front of the wafer at 5000 rpm for 30 seconds. The polyimide (DuPont PI-2555) was then spun on the front side of the wafer as its polyamic acid precursor from solution in N-methylpyrrolidone at 2000 rpm for 120 seconds, resulting in a polyimide thickness after cure of approximately four microns. The polyamic acid was baked at 120 °C for 10 minutes to drive off solvent and induce partial imidization and reaction with the adhesion promoter. Photoresist (KTI 820-20) was then spin-coated at 2500 rpm for 30 seconds on top of the polyimide and baked at 90 °C for 25 minutes. The supporting beams were patterned in the photoresist and the partially imidized polyimide simultaneously by the resist developer (a solution of tetramethylammonium hydroxide in water) (Fig. 2d). The resist was then stripped using acetone and methanol and the patterned polyamic acid beams were fully imidized by baking at 400 °C in nitrogen for 45 minutes. Finally, the wafers were blanket etched from the back using a sulfur hexafluoride plasma etch until the silicon in the trenches surrounding the plates was etched away, releasing the center plates.

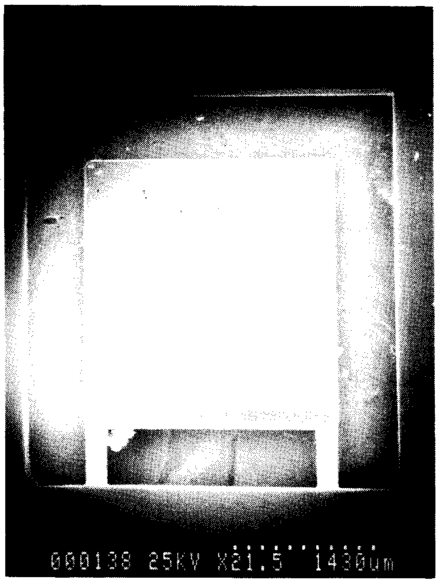

Figure 3. SEM photograph of suspended plate (bending beam design)

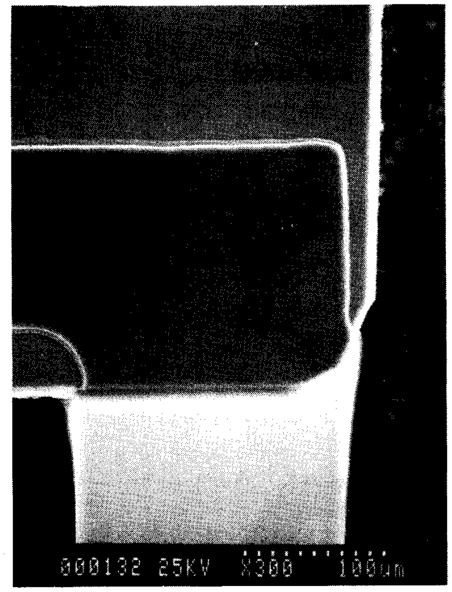

Figure 4. SEM detail of beam-plate junction (bending beam design)

Figure 3 shows a SEM photo of the fabricated structure. As can be seen, the plate is flat (unwarped) and supported only by the polyimide arms. The polyimide was removed in the plate fields so that residual stresses in the polyimide resulting from cure would not bend the plate. Figure 4 shows a detailed view of the supporting beam. Since the front-side trench etch is anisotropic, the polyimide can make the step over the plate and still keep the plate stable. Due to fabrication complications in this initial study, it was not possible to achieve the seven micron beam thickness required by the design goals, although thinner beams (down to 1 µm) could be achieved. As a result, it was found that the end torsional devices were most suitable for deflection purposes. Thus, the modelling and testing described below were limited to this configuration.

MODEL

A simple electromechanical model was used to relate applied voltage to expected deflection. Assuming the plate suspended over a ground (attracting) plane takes on the configuration of a parallel-plate capacitor (Figure 5), the force F acting on the plate due to an applied drive voltage V is given by:

$$F = \frac{\varepsilon_o A V^2}{2 h^2} \qquad (1)$$

where ε_o is the permittivity of the material between the plates (in this case, air); A is the area of attraction; and h is the separation distance between plates. This force is counterbalanced by the restoring force supplied by the supporting beams, which is calculated below [11].

For the prediction of the torsional restoring force of the polyimide beams, standard formulas have been used [12,13]. A point load is assumed to be acting on the moving plate (for these calculations, it is assumed that the position of the effective point load D is equal to half the plate length l_p)(Figure 5). It is further assumed that the plate remains rigid (all deflection occurring in the flexible beams), and that the effect of the residual tensile stress in the polyimide arms and the effect of the thin aluminum overcoat on the torsional restoring force can be neglected. These assumptions (especially the latter two) may not be fully justified, but were used to generate an initial model for the deflections involved. More sophisticated analyses are presently underway.

Under the above assumptions, it can be shown that the angle of deflection θ can be related to the applied point load P by [11]:

$$\theta = \frac{3 l P D (1+\nu)}{2 E a b^3 [16/3 - 3.36(b/a)]} \qquad (2)$$

where E and ν are the Young's modulus and Poisson's ratio of the beam, l is the length of the beam, and the quantities a, b, and D are defined in Figure 5. Combining equations (1) and (2) and realizing that the force to pull down the plate is twice P (since there are two beams), and that for small angles, the deflection of the tip of the plate is equal to the product of the angle of rotation θ and the length of the plate l_p yields the voltage-deflection relation:

$$d = \frac{3\,\varepsilon_o\,A V^2\,l\,D\,(1+\nu)\,l_p}{8\,h^2\,E\,a\,b^3\,[16/3 - 3.36(b/a)]} \qquad (3)$$

Thus, equation 3 predicts that a plot of d/V as a function of V should be linear, passing through the origin with slope m equal to:

$$m = \frac{3\,\varepsilon_o\,A\,l\,D\,(1+\nu)\,l_p}{8\,h^2\,E\,a\,b^3\,[16/3 - 3.36(b/a)]} \qquad (4)$$

As all of the quantities on the right hand side of Equation 4 are known, a direct comparison between the slope of the appropriately plotted voltage-deflection data and the prediction of equation (4) can be made.

TESTING

In order to test the flexibility of the devices, the wafers were broken into individual devices and coated with a thin (3000 Å) layer of aluminum using a filament evaporator. The device under test was placed over a ground plane and probed so that a voltage difference could be applied between the top surface of the plate and a ground plane underneath the plate. The test apparatus consisted of a probe station which had a height measuring device attached to the microscope head. As the plates were electrostatically deflected, the microscope focus had to be changed in order to keep the tip of the plate in view. Changing the focus moved the microscope head and thus allowed the determination of the deflection of the plate tip as a function of the applied voltage. Figure 6 shows a plot of the voltage-deflection data collected in this manner. The results are fairly reproducible on the same sample, although there is some variation from sample to sample. Figure 7 is a plot of d/V vs. V, as suggested by the theoretical calculations. As can be seen, we do observe a reasonably straight line (scatter is more pronounced at small deflections due to errors in deflection measurement). The best-fit slope of the line is 4.78×10^{-2} $\mu m/V^2$, in fair agreement with the value calculated from Equation 4 of 3.9×10^{-2} $\mu m/V^2$ (see Table I). The best-fit line does not pass through the origin, however, indicating the presence of a term linear in voltage which does not appear in Equation 3. There are several possible reasons for this discrepancy. One possibility is that the simple electromechanical model is insufficient to describe the forces acting on the plate. Other reasons could lie in the beams themselves. The polyimide beams are quite small, and any overetching will therefore make a large difference in the beam dimensions and change their mechanical characteristics (values of fabricated beam widths as measured in the SEM as opposed to drawn beam widths were used in Equation 4 to minimize this difficulty; this is the entry given in Table I). In addition, the beams do not have a uniform cross-section along their lengths. Extra stresses have also been introduced by the aluminum coating on the top side of the devices. Finally, the residual tensile stress in the polyimide beams may be affecting the beam behavior. In spite of these many difficulties, the simple theory and the measured behavior of the fabricated devices are not radically different.

In another test, one of the mirrors was used to deflect a laser beam in order to determine the reflectivity and mechanical resonant frequency of the plate. An incident beam was focussed on the mirror plate which reflected the beam to a spot on the room ceiling. Application of electrostatic voltage to the mirror caused a change in position of the ceiling spot, which was reversible when the drive voltage was removed. By measuring the maximum travel of the spot, the maximum mirror deflection was calculated to be approximately six degrees. Additional tests showed that the mirror could be driven into mechanical resonance by modulating the electrostatic drive voltage with a square or sine wave drive from a function generator. By scanning the frequency of the drive voltage, a maximum in the plate deflection of approximately 1.4 times the low-frequency deflection could be observed at a frequency of 112 Hz.

CONCLUSIONS

A new type of micromachined structure, large silicon plates suspended entirely by insulating and flexible polyimide beams, has been fabricated. The fabrication sequence allows the integration of electronic devices on the wafer or plate if so desired. The structures have been deflected electrostatically at reasonable voltages and can be driven into resonance. The reflection position of laser beams incident on the plates can be adjusted electrically by changing the electrostatic drive voltage (and thus the position) of the plate. The electrostatic behavior of these structures has been found to be in fair agreement with a simple electromechanical theory. These structures were designed for application as micromachined mirrors, although their sensitivity to motion and electrical and thermal isolation suggest other potential applications such as gas sensors, flow sensors, and accelerometers.

Table I. Beam parameters used in Equation (4)

Parameter	Description	Value
A	plate area	4 mm^2
l_p	plate length	2 mm
l	beam length	0.5 mm
D	effective force position	1 mm
h	plate separation	0.3 mm
a	beam half width	40 µm
b	beam half thickness	2 µm

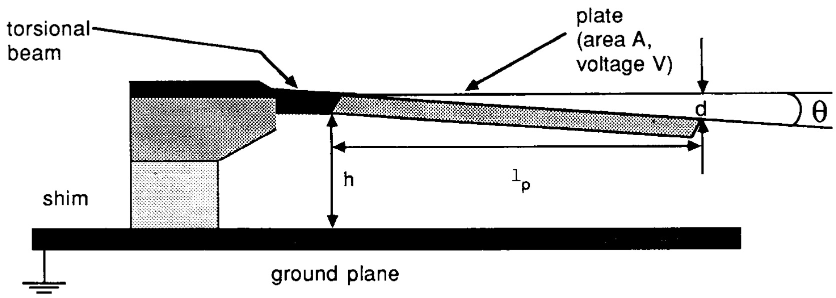

Figure 5. Definition of parameters for plate under test
(The shim under the wafer is only used for resonance testing)

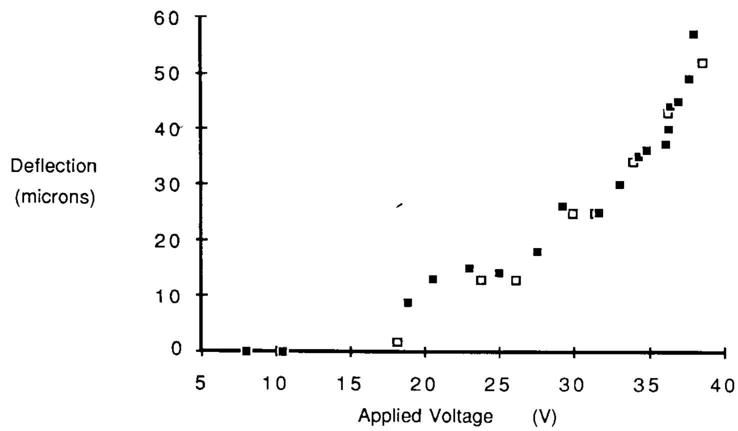

Figure 6. Tip deflection versus voltage for an end torsional plate. Open squares - run 1; closed squares, run 2

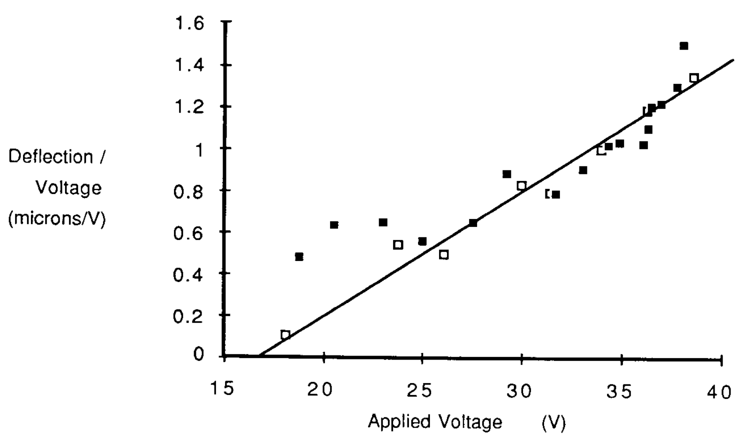

Figure 7. Tip deflection divided by voltage versus voltage for an end torsional plate. Open squares - run 1; closed squares, run 2. Line represents linear best fit to data in accordance with Equation 3.

ACKNOWLEDGEMENT

This paper arose from a project undertaken as part of MIT subject 6.151 (Semiconductor Devices Project Laboratory). One of the authors (MGA) is supported in part by a graduate fellowship from the International Society for Hybrid Microelectronics. Microfabrication was carried out in the Microsystems Technology Laboratories, the MIT Microelectronics Educational Facility, and the Microelectronics Laboratory of the MIT Center for Materials Science and Engineering, which is supported in part by the National Science Foundation under contract DMR-84-18718. Assistance from Douglas Young in sample fabrication is gratefully acknowledged. The authors would like to thank Professor Martin Schmidt for helpful technical discussions and Professor Stephen Senturia for his support of this project and for providing a critical reading of the manuscript.

REFERENCES

1. K.E. Petersen, 'Silicon Sensor Technologies', in IEDM Technical Digest, 1985, p.2
2. W. Riethmueller and W. Benecke, 'Thermally Excited Silicon Microactuators', IEEE Transactions on Electron Devices **35**, p. 758-762 (1988)
3. K.E. Petersen, 'Micromechanical Membrane Switches on Silicon', IBM J. Res. Dev., **23**, p. 376 (1979)
4. L.J. Hornbeck, '128x128 Deformable Mirror Device', IEEE Transactions on Electron Devices **ED-30**, p. 539-545 (1988)
5. K. Gustafsson and B. Hoek, 'Fiberoptic Switching and Multiplexing with a Micromechanical Scanning Mirror', in Proceedings of the Fourth International Conference on Solid State Sensors and Actuators, *Transducers '87*, p. 212-215
6. K.E. Petersen, 'Silicon Torsional Scanning Mirror', IBM J. Res. Dev., **24**, p. 671 (1980)
7. K.E. Petersen and C.R. Guarnieri, 'Micromechanical Light Modulator Array Fabricated on Silicon', Appl. Phys. Lett., **31**, 521 (1977)
8. G. Stemme, 'An Integrated Gas Flow Sensor with Pulse-Modulated Output', in Proceedings of the Fourth International Conference on Solid State Sensors and Actuators, *Transducers '87*, p. 364-367
9. M. G. Allen, M. Mehregany, R.T. Howe, and S.D. Senturia, 'Microfabricated Structures for the *in-situ* Measurement of Residual Stress, Young's Modulus, and Ultimate Strain of Thin Films', Appl. Phys. Lett., **51**, 241 (1977)
10. M. Mehregany, R.T. Howe, and S.D. Senturia, 'Novel Microstructures for the *in-situ* Measurement of Mechanical Properties of Thin Films', J. Appl. Physics **62**, 3579 (1987)
11. M. Scheidl, 'The Design and Fabrication of Movable Micromachined Mirrors', S.B. Thesis, Department of Mechanical Engineering, Massachusetts Institute of Technology, May, 1988
12. J.N. Goodier, 'Torsion', in Handbook of Engineering Mechanics, W.L. Fluegge (ed.), McGraw Hill, New York, 1962
13. R.J. Roark and W.C. Young, Formulas for Stress and Strain, McGraw Hill, New York, 1975, p. 290